International Journal of Energy
ISSN: 2957-9473 | Vol. 3, No. 3, 2023

Study on Evolution Characteristics of Stress Field of Stepped Fault

Guangsheng Chen *

School of Energy Science and Engineering, Henan Polytechnic University, Jiaozuo, Henan, 454003, China

*** Corresponding author Email:** 18836413761@163.com

Abstract: With the development of mining to the deep, the ground stress increases correspondingly, and the geological conditions become more and more complicated. Mine dynamic disasters mainly occur near faults. Numerous studies have been conducted on single faults, but few studies have been done on stepped faults formed by double faults under complex geological conditions. Based on this, with the 3110-working face of Zhong Tai Mining in He bi as the engineering background, Single fault model a and different step fault models b, c, d, e and f were established by Flac3D numerical simulation software. The characteristics of stress field evolution of single fault and step fault under the influence of deep mining are studied. The results show that the stress distribution in the upper wall of the fault forms a stress concentration zone, and in the lower wall forms a stress weakening zone. Under the influence of excavation disturbance, the vertical fault distance and the horizontal distance between faults will affect the stress evolution characteristics of the stepped fault.

Keywords: Step Fault; Ground Stress; Stress Concentration; Evolutionary Characteristics; Flac3D Numerical Simulation.

1. Introduction

With the increase of coal mining depth, the ground stress continues to rise, and the state of ground stress is gradually transformed from the shallow tectonic stress to the deeper two-direction isobaric state and the ultra-deep three-direction isobaric stress state.[1,2]At the same time, the existence of geological structural phenomena will lead to changes in the continuity of rock mass and the stress field of primary rock. With the advance of the working face, the damage and fracture of the fault will be intensified under the influence of the mining of the working face during the process of approaching and passing through the fault, resulting in fault activation, which is significantly different from the normal mining phenomenon [3,4]Typical dynamic disasters such as coal and gas outburst and rock burst are easily induced under mining activities [5-9]It is of great significance to study the distribution of mining stress in fault tectonic area for mine dynamic disaster prevention.

Domestic and foreign scholars have conducted many studies on the influence of faults on fully mechanized mining working faces. Shi Guilin et al.[10,11]studied the evolution law of stress field under different fault dip angles by using the research method of combining physical similarity simulation and PFC numerical simulation. It is found that the increase of fault dip Angle will cause the fault failure form to change from the slide failure at low Angle to the shear failure at high Angle and will induce the stress increasing area to move from bottom to up. Zhang Chen et al. [12,13]used the numerical simulation analysis method to study different fault dip angles under the effect of double fault superposition, and found that the leading stress of the working face reached its peak earlier under the condition of superposition and high dip Angle. Jiao Zhenhua et al.[14]established a numerical model of working face crossing faults and analysed that the damage slip of faults under mining disturbance was mainly affected by horizontal stress, internal friction Angle of faults and distance from the working face. Wang Hongwei et al [15]established a mechanical model of fault structure and a physical model of the occurrence of thick roof under the influence of mining, and systematically expounded the mechanical mechanism of fault structure instability and the multi-physical field precursor characteristics of fault instability induced thrust. Jiang Jinquan et al.[16]used Flac3D numerical simulation to study the evolution characteristics of mining stress when the working face is advancing towards normal fault and the working face is arranged along normal fault, and concluded that there is an "inverted wedge" stress zone between the working face and fault, and a "wedge" stress zone in the overlying rock outside the fault. Wang Xuebin et al.[17] used the Flac3D numerical simulation method to study the barrier effect of fault on mining stress during the advancing process of normal fault footwall working face. Dong Shuangyong et al.[18] used the combination of internal and external stress field theory and numerical simulation to calculate and study the influence of principal stress deflection on fault stability during working face excavation of normal fault footwall. Yu Qiuge et al.[19,20]used the Flac3D numerical simulation method to study the influence of parameters such as water content or not in the fault zone and elastic modulus of rock mass in the fault zone on fault activation. Based on field monitoring and observation, Shan et al.[21]found that the working face parallel to the strike of the fault is prone to intense fault activation during mining, and the fault slip risk is related to the percentage of stress unloading of the lateral principal stress and axial principal stress, and is particularly sensitive to the unloading amount of the lateral principal stress.

This paper is based on the geological conditions of 3110 working face of 21 Coal seam of Zhong Tai Mining in He bi, and the buried depth of coal seam in the working face is as follows: 520.6m ~ 644.3m, this working face belongs to coal pillar working face, the surrounding goaf gas has been released, 3110 working face is expected to expose 3 faults. Flac3D numerical simulation method is used to study the evolution law of mining stress on deep stepped faults affected by mining.

2. Model Building

2.1. Model Parameter Settings

Based on the analysis of the borehole column chart of Zhong Tai Mining Company, the direct roof of the working face is set to be gray-black mudstone, the main roof is dark-grey layered medium-grained quartz sandstone, the direct floor is grey-white giant thick layered fine-grained quartz sandstone, and the main floor is grey-black sandy mudstone.

This numerical simulation test is mainly aimed at studying the evolution characteristics of stress field, weakening the mechanical properties of rock in the fault zone, and adopting the impact test data of drilling lithology in the laboratory for the physical parameters of coal strata, whose mechanical parameters are shown in Table 1:

Table 1. Material mechanical parameters of the numerical simulation model.

Type	Density /kg·m^{-3}	Bulk /GPa	Shear /GPa	friction /°	Cohesion /MPa	Tensile /MPa
Medium grained sandstone	2748	21.70	10.60	25	2.50	3.04
Mudstone	2576	6.32	3.61	29	1.30	1.59
Coal	1459	8.82	3.38	19	1.20	1.20
Fine grained sandstone	2706	22.79	10.52	30	2.80	2.70
Sandy mudstone	2604	8.29	5.21	28	1.90	1.67
Fault	2000	1.79	0.55	11	0.30	0.02

2.2. Model Building and Initial Condition Setting

This test is based on the geological conditions of the 3110-working face of the second1 coal seam of Zhong tai Mining Company. The model is 150m long, 50m wide and 60m high. The old top thickness is 10m medium grained sandstone, the direct top thickness is 7m mudstone, the coal seam thickness is 8m, the direct bottom thickness is 5m fine grained sandstone, and the base thickness is 30m sandy mudstone. The fault is stepped, and the lower end disappears at the base of the coal seam, and the thickness of the fault weakening zone is about 1.5m. The working face is mined from the footer, and the mining method is adopted to strike the longwall and drop coal mining, with a mining height of 3m. According to relevant studies, when the coal roadway is driven from the foot, when the driving distance is within 50 meters of the fault plane, the high value area of vertical, horizontal and shear stress near the coal wall of the working face is close to the fault and affected by the fault barrier effect, and the influence effect is intensified[17] within 20m. Therefore, the original stress field and the stress state of the model 30m, 20m, 10m and 5m away from the fault were recorded. The related parameters of rock mass faults are shown in Table 2:

Table 2. Fault parameters of rock mass

Type	Fault 1 Dip /°	Fault 2 Dip /°	Fault1 spacing/m	Fault1 spacing/m	Double fault spacing/m
Fault a	60	-	4	-	-
Fault b	60	60	4	4	50
Fault c	60	60	4	6	50
Fault d	60	60	4	8	50
Fault e	60	60	4	4	40
Fault f	60	60	4	4	30

Assuming that the rock mass is a uniform continuous medium, the Moore-Coulomb elastoplastic model is adopted, and the whole model is cuboid. The grid surfaces of the model are grouped into West, East, North, South, Top and Bottom respectively (Figure 1). Displacement constraints are set for the West, East, North, South and Bottom mesh surfaces. In the gravity stress field of rock mass, the vertical stress σ_z, the average Poisson ratio of rock is 0.29, and the horizontal stress σ_x, σ_y of rock mass are about 40% of the vertical stress, as shown in Formula (1) and (2).

$$\lambda = \frac{\mu}{1-\mu} \tag{1}$$

$$\sigma_x = \sigma_y = \lambda\sigma_z \tag{2}$$

Where: λ is the side pressure coefficient, μ is the rock Poisson ratio.

Where, if the average density of rock mass is 2.6 × $103Kg/m^3$, and the acceleration of gravity is 10m/s^2, it is necessary to apply 15.6MPa vertical stress on the Top surface of the model grid. The model establishment is shown in Figure 1:

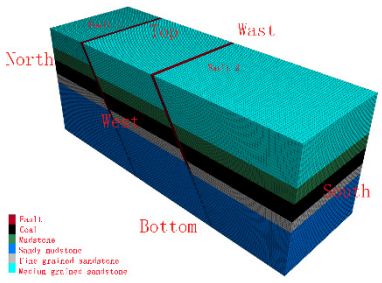

Figure 1. Step fault b model diagram.

3. Simulation Results

According to the above conditions, the height and width of the coal seam roadway are set to be 3 meters, and the excavation starts from the foot of the fault, 37m away from the initial distance of the fault.

3.1. Original Stress Simulation Results

The initial ground stress state cloud map of each fault before excavation is shown in Figure 2:

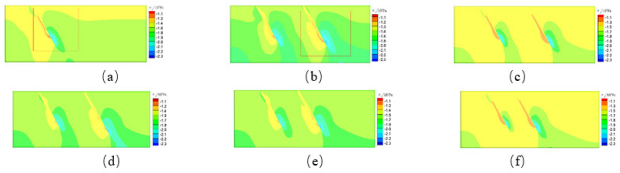

Figure 2. Initial ground stress map of each fault before excavation.

3.2. Stress Simulation Results after Excavation

In order to study the influence of excavation and mining process on ground stress, the stress field characteristics at the position 30m, 20m, 10m and 5m away from the fault at the working face are observed. The stress cloud diagram of the simulated results of each fault is shown in Figure 3:

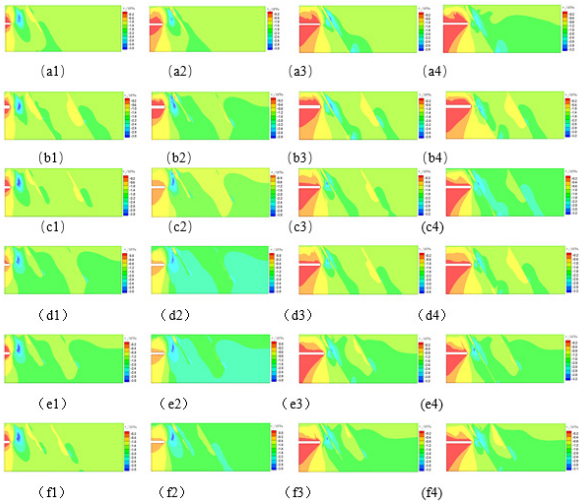

Figure 3. Stress evolution cloud map of each fault after excavation.

4. Analysis of Stress Field Evolution Law

The maximum stress value in the evolution process of stress field is taken, and the maximum initial stress of each fault, the maximum stress of single fault and stepped fault under the mining disturbance and the maximum stress of different stepped fault under the influence of mining are compared and studying the stress evolution law. Each maximum value is shown in Table 3.

Table 3. The maximum ground stress value when working face is at different distance from the fault.

Items	37m /MPa	30m /MPa	20m /MPa	10m /MPa	5m /MPa
Fault a	22.7	30.25	29.33	27.63	30.27
Fault b	22.7	31.41	29.06	27.46	31.05
Fault c	22.6	31.79	30.77	31.7	31.63
Fault d	22.95	30.83	30.6	33.82	31.4
Fault e	22.61	31.58	31.51	33.63	31.7
Fault f	22.56	31.89	31.41	32.69	31.64

4.1. State of Initial Ground Stress

Without the influence of mining disturbance, as shown in FIG. 3 and FIG. 5, the influence of single fault and stepped fault on initial ground stress mainly has the following characteristics:

(1) Stress distribution in the upper wall of the normal fault is the stress strengthening zone, and the lower wall is the stress weakening zone. At the same time, the fault is bounded, and the stress concentration zone is formed in the upper wall of the fault.

(2) The stress distribution on the right side of single fault a is very similar to that on the right side of step fault b, as shown in Figure 3 (a) and (b), the maximum ground stress is 22.7MPa. The fault on the left side of fault b is affected by the weakening of fault barrier to stress, and a decreasing stress circle from left to right is formed in the weakening zone of fault footwall, while an increasing stress circle from right to left is formed in the upper wall.

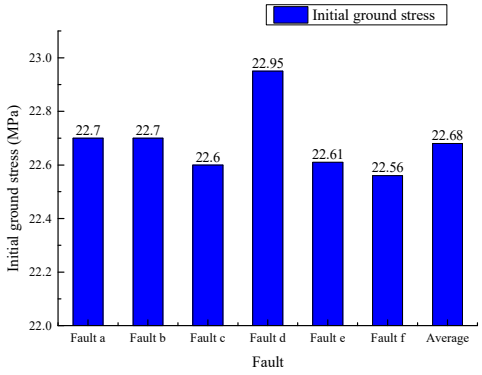

Figure 4. Histogram of maximum initial ground stress of different faults.

(3) Compared with step fault b, c and d, when the vertical fault distance of the right fault increased from 4 meters to 8 meters, the maximum ground stress showed an increasing trend, and the maximum ground stress was 22.95MPa on step fault d.

(4) Compared with step faults b, e and f, when the distance between the two steps is reduced from 50m to 30m, the maximum ground stress shows a decreasing trend, and the minimum value is 22.56MPa of step fault f

4.2. Evolution Law of Ground Stress Field in the Process of Excavation

In the process of excavation, as shown in Figure 4 and Figure 5, the stress field changes as the working face gradually approaches the fault, and its main characteristics and laws are as follows:

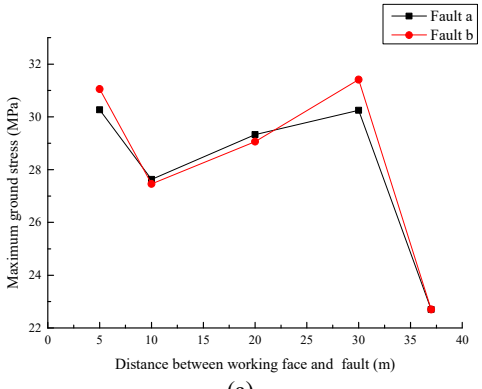

(a)

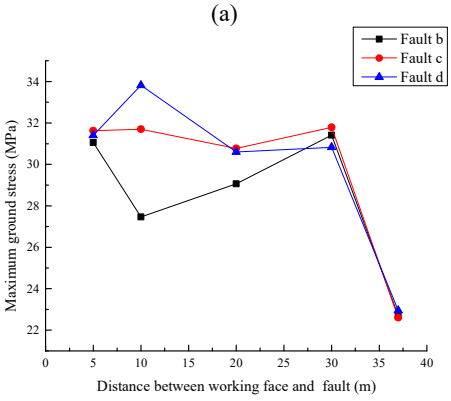

(b)

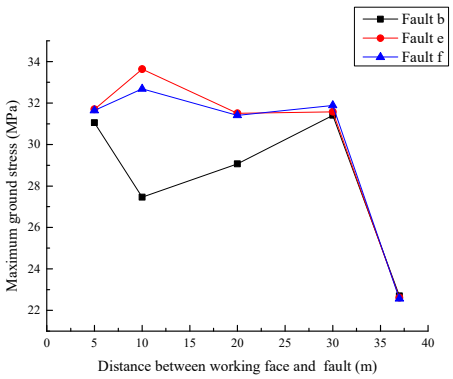

(c)

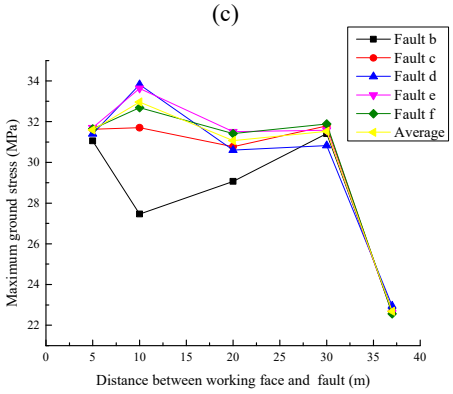

(d)

Figure 5. Line chart of maximum stress values of different faults during excavation

(1) There is always a stress concentration zone about 10m in front of the working face in the process of excavation, and the stress concentration zone gradually approaches the fault in the process of forward excavation, and the stress concentration area becomes smaller when it crosses the fault, and the stress concentration phenomenon is more obvious. For step faults, the evolution of stress concentration zone is lagging compared with that of a single fault.

(2) In the process of advancing the distance from the working face to the fault from 30m to 20m, the stress concentration area changes from a large area of water droplets to a small area of strips.

(3) Before the stress concentration area passes through the fault, the phenomenon of stress concentration becomes more and more obvious with the reduction of the distance between the working face and the fault. At the same time, after the stress concentration area passes through the fault, the stress concentration phenomenon slows down.

(4) Figure. 6 (a) shows that the threshold value of maximum ground stress change is larger for stepped faults and single faults, and the overall change of both faults is a trend of first increasing, then decreasing and then increasing.

(5) Figure 6 (b) shows the process of the vertical fault distance of step fault 2 changing from 4m to 8m. When the excavation reaches 20m, the maximum ground stress of step fault c and d increases in reverse. It is shown in the figure that the maximum ground stress increases with the increase of vertical fault distance. And when the excavation reaches 5m, the maximum ground stress of b, c and d faults tends to be about 31MPa.

(6) Figure.6 (c) shows that when the distance between step faults 1 and 2 is reduced from 50m to 30m, the maximum ground stress also increases in the reverse direction, and the extreme points of their respective changes appear at 10m. With the reduction of the distance between faults, the change of the maximum value is first large and then small, and the maximum value is 33.63MPa of 40m distance between faults.

(7) The maximum ground stress values of the stepped faults c, d, e and f were normalized, as shown in Figure 6 (d) yellow line. The maximum ground stress changed from the "N" type of the original blue line to the "M" type of the yellow line with the changing trend of the excavation process.

5. Conclusion

(1) Without the influence of mining disturbance, there is no significant difference between the maximum original ground stress of step fault and that of a single fault. The stress distribution of step fault 2 is very similar to that of a single fault. The stress distribution of step fault 1 is affected by fault 2, and the stress value of the stress weakening area of the fault footwall is smaller.

(2) When the excavation surface of the stepped fault is 20 meters away from the fault, the stress concentration area changes from "droplet" to "strip" in the fault footwall, and the stress concentration phenomenon is intensified; When the driving face is 10m away from the fault, the stress concentration area of single fault a and step fault b crosses the fault. Affected by the vertical fault distance and the distance between faults, the stress concentration area of fault c, d, e and f is tightly attached to the fault footwall, and the stress concentration reaches the maximum value, which is 33.82MPa of fault d.

(3) With the increase of vertical fault distance, the maximum ground stress of step fault 2 also shows an increasing trend; When the distance between fault 1 and fault 2 is shortened, the maximum ground stress value firstly increases and then decreases. Under the disturbance of mining and excavation, the maximum ground stress of step fault changes from "N" type to "M" type.

(4) When the excavation surface is 5m away from the fault, the stress concentration area basically passes through fault 1, and the maximum ground stress value of all models is about 31MPa. This indicates that under the influence of mining, the propagation of the stress field of the stepped fault has the effect of accumulation and superposition. When the stress concentration area does not cross the fault, the stress superposition state is mainly manifested, and the maximum stress is also increased. At the same time, the increase of the vertical fault distance of the fault or the shortening of the spacing between faults will delay the time of the stress concentration area crossing the fault. When the stress concentration area passes through the fault, the stress is redistributed, and the stress field returns to a relatively consistent phenomenon.

References

[1] Tong qing Chen. Research on Three-dimensional Stress Evolution Characteristics of Mining Coal and Rock and Its Influence on Rock Burst [D]. China University of Mining and Technology, 2021.

[2] He ping Xie, Feng Gao, Yang Ju, et al. Quantitative definition and investigation of deep mining [J]. Journal of China Coal Society, 2015, 40(01): 1-10.

[3] Wen ke Zhang, Gang Yang, Zhi qiang Li. Study on fault activation induced shock mechanism under the influence of mining[J]. Energy Technology and Management, 2023, 48(01): 61-64.

[4] Zhan shuo Wang. Experimental study on fault activation conducting water inrush [D]. China University of Mining and Technology, 2022.

[5] Lin ming Dou, Xin yuan Tian, An ye Cao, et al. Present situation and problems of coal mine rock burst prevention and control in China [J]. Journal of China Coal Society, 2022, 47(01): 152-171.

[6] Chuan zhi Jia. Control effect of structure on rock burst[J]. Heilongjiang Science and Technology Information, 2017, (12): 87.

[7] Liang Yuan. Research progress on risk identification assessment monitoring and early warming technologies of typical dynamic hazards in coal mines [J]. Journal of China Coal Society, 2020, 45(05): 1557-1566.

[8] Liang Yuan. Research progress of mining response and disaster prevention and control in deep coal mines [J]. Journal of China Coal Society, 2021, 46(03): 716-725.

[9] Ran Bao, Kai Li. Simulation Study on Effect of Fault Throw on Activation of lnverse Fault[J]. Safety in Coal Mines, 2017, 48 (05): 46-48.

[10] Jia lin Shi, Qian ting Hu, Yong jiang Luo, et al. Study on evolution law of fault stress field in coal measures at different fault dips [J]. Mining Safety & Environmental Protection, 2023, 50(01): 1-8.

[11] Qing xin Qi, Yi shan Pan, Hai tao Li, et al. Theoretical basis and key technology of prevention and control of coal-rock dynamic disasters in deep coal mining [J]. Journal of China Coal Society, 2020, 45(05): 1567-1584.

[12] Chen Zhang, Rong rong Cao, Kun Jia. Mining Stress Distribution Characteristics of Different Fault Dip Angles under Influence of Fault Superposition [J]. Coal Technology, 2022, 41(09): 71-74.

[13] Quan sen Wu, Li shuai Jiang, Peng Kong, et al. Effects characteristics of fault pillar and its dip angle on mining-induced stress and energy distribution[J]. Journal of Mining & Safety Engineering, 2018, 35(04): 708-716.

[14] Zhen hua Jiao, Yao dong Jiang, Yi xin Zhao, et al. Study of dynamic mechanical response characteristics of working face passing through reverse fault [J]. Journal of China University of Mining & Technology, 2019, 48(01): 54-63.

[15] Hong wei Wang, Qing Wang, Rui ming Shi, et al. A review on the interaction mechanism between coal bursts and fault structure instability from the perspective of multi-physical field[J]. Journal of China Coal Society, 2022, 47(02): 762-790.

[16] Jin quan Jiang, Quan lin Wu, Hua Qu. Evolutionary characteristics of mining stress near the hard-thick overburden normal faults [J]. Journal of Mining & Safety Engineering, 2014, 31(06): 881-887.

[17] Xue bin Wang, Zhang sheng Guo, Chao qun Deng. Numerical modeling of fault barrier effects on three kinds of stresses: a case of footwall mining on the normal fault [J]. Progress in Geophysics, 2020, 35(04): 1605-1611.

[18] Shuang yong Dong, Wen zhou Li. Influence analysis of principal stress deflection on fault stability based on theory of internal and external stress fields [J]. Safety in Coal Mines, 2021, 52(01): 213-219.

[19] Qiu ge Yu, Hua xing Zhang, Yu jun Zhang, et al. Analysis of fault activation mechanism and influencing factors caused by mining [J]. Journal of China Coal Society, 2019, 44(S1): 18-30.

[20] Guang li Zhu, Wen quan Zhang, Gui bin Zhang, et al. Experimental study on fault activation conducting water inrush [J]. Rock and Soil Mechanics, 2017, 38(11): 3163-3172.

[21] Renliang Shan, Liu Dong, Wang Hailong, et al. Study of the fracture instability and fault slip risk of overlying strata during mining near faults[J]. Bulletin of Engineering Geology and the Environment, 2023, 82(3): 82-94.